

Interrelationships between snowpack dynamics and tree growth in the Tigiretsky Ridge (Altai): Implications for ecological responses to climate variability

Nikolay I. Bykov¹, Roman Ju. Birjukov¹

1 Institute for Water and Environmental Problems, Siberian Branch, Russian Academy of Sciences, 1 Molodeznaya St., Barnaul, 656038, Russian Federation

Corresponding author: Nikolay I. Bykov (nikolai_bykov@mail.ru)

Academic editor: A. Matsyura | Received 5 October 2024 | Accepted 1 November 2024 | Published 20 November 2024

<http://zoobank.org/1EC9CEC6-48E2-412D-83AB-ADED806F4646>

Citation: Bykov NI, Birjukov RJu (2024) Interrelationships between snowpack dynamics and tree growth in the Tigiretsky Ridge (Altai): Implications for ecological responses to climate variability. *Acta Biologica Sibirica* 10: 1319–1336. <https://doi.org/10.5281/zenodo.14190443>

Abstract

This study examines the complex interplay between snowpack dynamics and tree growth in the Tigiretsky Ridge region, utilizing a combination of tree-ring chronologies and snowpack data from 2013 to 2020. Employing the Temperature-Based Melt-Index Method, we accurately assessed the maximum snowpack water equivalent during winter months, revealing significant spatial variability influenced by elevation, slope aspect, and proximity to watersheds. Our findings indicate an asymmetrical distribution of snow cover, with higher snow reserves on the southern slopes at lower elevations and a reversal at higher altitudes. Notably, near watershed areas, snow reserves on the northern slope can exceed those on the southern slope by a factor of 30. The analysis also highlights the positive correlation between increased snowpack water equivalent and radial growth of *Abies sibirica* L. within the ecotone of the upper timberline, suggesting a significant ecological response to changing snow conditions. These insights contribute to a deeper understanding of how climate variability impacts snow-vegetation interactions in mountainous ecosystems, laying the groundwork for future research aimed at unraveling the underlying mechanisms of these relationships.

Keywords

Altai, Tigiretsky Ridge, snow cover, Temperature-Based Melt-Index Method, tree rings, woody plants

Introduction

Snow cover is a crucial ecological component that influences both biotic and abiotic factors within ecosystems. Its high reflectivity alters surface albedo, while its insulating properties affect heat transfer rates between the soil and atmosphere, impacting soil freezing depth and overall energy balance in the area. Additionally, snow cover plays a pivotal role in the water regime of ecosystems in various regions worldwide, dictating river flow, soil moisture, and more. By modifying hydrothermal conditions, snow cover influences the life processes of plant and animal species, affecting their spatial and temporal distribution, productivity, and phenology (Nefedeva, Yashina 1985).

However, snow cover observations conducted by meteorological services are often limited to localized areas. At best, these observations can only be correlated with zonal natural structures. This issue is particularly pronounced in mountainous regions, where the labor-intensive nature of ground-based snow measurements increases alongside the number of variables affecting snow distribution, such as altitude, slope exposure, and ridge orientation relative to air mass transport. Consequently, these challenges hinder the quantitative assessment of the ecological significance of snow cover and complicate predictions regarding ecosystem states in the context of climate change.

The rapid advancement of remote sensing technology is providing solutions to many of these challenges. Satellite imagery enables the assessment of snow cover phenology and its spatial distribution at specific time points (Hao et al. 2022; Jing et al. 2022; Zschenderlein et al. 2023). This capability allows for the transition to quantitative indicators of snow cover, including the mapping of snow extent, assessment of snow duration, and ultimately, the estimation of snow water reserves.

Various approaches exist for estimating snow water reserves, with one of the most widely used being the Temperature-Based Melt-Index Method (Glaciological Dictionary 1984). This method quantifies the relationship between air temperature and the amount of snowmelt in water equivalent. Specifically, it defines the melting temperature coefficient as the amount of water equivalent (in millimeters) generated per day for every degree Celsius of positive average daily temperature. Historically, the relationship between melting rates and air temperature was first substantiated by Hann (1908) and Ahlmann (1924) in their investigations of glacial altitudes. The method was later adapted in the USSR by researchers such as Krenke and Khodakov in 1966, and further studies (Kotljakov et al. 1981) reinforced its relevance. Today, this method continues to be applied in hydrological and glaciological studies (Reeh 1989; Lang and Braun 1990; Braithwaite 1995; Hock 1999), including in the Altai region (Iglorskaya, Narozhny 2010).

Improvements to the method typically involve incorporating additional variables such as solar radiation and wind (Lang 1978). However, research by Ohmura (2001) demonstrates that these enhancements can complicate calculations and may require data that are not consistently available. The primary advantages of the Tem-

perature-Based Melt-Index Method lie in its accuracy, the widespread availability of air temperature data, and its straightforward spatial interpolation capabilities.

The necessity of employing this method in the Altai mountainous region stems from the limited availability of ground-based weather stations. Most of these stations are situated in valley bottoms at lower altitudes, providing an incomplete representation of snow cover distribution across varying elevations. This limitation complicates our understanding of how snow cover influences altitudinal zonation, vegetation productivity, and other related factors.

In light of these considerations, the aim of our study is to establish quantitative indicators of snow cover on the Tigiretsky Ridge by utilizing seasonal snow line data obtained through remote sensing. We will identify the geographical distribution of snow cover and analyze its impact on vegetation productivity.

Materials and methods

The study area encompasses the western part of the Tigiretsky Ridge and its adjacent regions, including the basins of the Ini and Belaya rivers (tributaries of the Charysh River) located in Russia, and the Beloporozhnaya Uba River (a tributary of the Uba River) in Kazakhstan. This landscape is classified as mountainous, characterized by low- and medium-mountain subclasses ranging from 500 to 2000 meters above sea level (m a.s.l.), along with intermountain-basin subclasses (Chernykh, Samoilova 2011). The primary landscape types in the region include tundra, alpine meadows, forests, and forest-steppe, with forests covering approximately three-quarters of the area. Notably, this region marks the northwestern edge of the Altai Mountain Region.

Winter precipitation is primarily associated with cyclones linked to the Arctic front, contributing to 85 to 90% of total snowfall in the study area (Egorina, Revyakin 2022; Climate... 2009). The Tigiretsky Ridge acts as a barrier to the westward movement of air masses; some of these masses are partially diverted, resulting in a “barrier shadow” effect (Egorina 2003). This phenomenon leads to reduced precipitation levels in the Tigirek-Inskaya basin compared to other areas at similar altitudes. For instance, snow depth and snowpack water equivalent at Tigirek (480 m a.s.l.) consistently fall short of values observed in Zmeinogorsk (354 m a.s.l.), Shemonaiha (320 m a.s.l.), and the Marinikha Cordon of the Tigirek Reserve (490 m a.s.l.) (see Fig. 1). This discrepancy is not only due to lower precipitation but also influenced by föhn winds, which can trigger thawing conditions.

Snowpack water equivalent increases significantly with altitude. Instrumental observations indicated that in February 1988, the maximum snowpack water equivalent reached 138 mm at an altitude of 354 m in Zmeinogorsk (with a 1991–2020 average of 125 mm), while at 1600 m, it soared to 982 mm (Bykov et al. 2024). In March 1987, the values were 213 mm and 1396 mm, respectively (Bykov et al. 2021). Other studies indicate that snow reserves at the upper timber line can exceed 1500

mm, and on leeward slopes, snow accumulations due to drifting can reach up to 5000 mm, corresponding to snow depths of 2 to 3 meters (Revyakin, Kravtsova 1977; Revyakin 1981). The gradients of maximum snow reserves in the Altai-Sayan region can vary from 15 to 100 mm per 100 m of altitude, with notably high values recorded in both our study area and the Kuznetsk Alatau.

This study aims to achieve several objectives: 1) identifying the position of snow cover during the spring and summer months using satellite data; 2) calculating the melting temperature coefficient based on Zmeinogorsk weather station data; 3) summing average daily air temperatures across varying altitudes for specific dates; 4) determining maximum snow reserves via the Temperature-Based Melt-Index Method across different altitudes; 5) creating a map depicting maximum snow reserves based on calculated figures and snow cover positions derived from satellite imagery; and 6) assessing the influence of snow cover indicators on the radial growth of trees.

The primary source of remote sensing information for this study was satellite imagery from Sentinel-2. This multispectral data, with spatial resolutions ranging from 10 to 60 meters across the visible, near-infrared (VNIR), and shortwave infrared (SWIR) spectral bands, comprises 13 spectral channels. We analyzed seven scenes from the active snowmelt period of 2021, specifically from May 2, May 4, May 24, May 29, June 6, June 16, and July 3. Images captured on other dates during the spring-summer period were excluded from analysis due to significant cloud cover.

For automated snow cover mapping, we employed the Normalized Difference Snow Index (NDSI), as described by Hall et al. (1995) and Hall and Riggs (2011). This index quantifies the difference in light absorption between the shortwave infrared (SWIR) and visible green regions of the electromagnetic spectrum:

$$\text{NDSI} = (\text{Green} - \text{SWIR1}) / (\text{Green} + \text{SWIR1}),$$

where "Green" represents reflectance in the green spectrum and "SWIR1" represents reflectance in the shortwave infrared region. After calculating the NDSI, we generalized the data using a majority filter with a threshold of 3 pixels to minimize errors along contour boundaries.

Terrain data was derived from the Forest and Buildings Removed Copernicus Digital Elevation Model (FABDEM), which provides global terrain information with a resolution of 30 meters between 60° south latitude and 80° north latitude. This dataset is based on the Copernicus DEM, with forest and building features removed.

To establish the temperature coefficient of melting specific to the region, we analyzed average daily air temperatures, daily precipitation amounts, and snowpack water equivalent data sampled on specific dates from the Zmeinogorsk weather station between 2013 and 2021 (Table 1). We also utilized data from automatic weather stations within the Tigirek Reserve, located at altitudes of 480 and 1530 m a.s.l.

These data were used to interpolate average daily temperatures for altitudes in between and then extrapolated up to 2000 m a.s.l.

Using the calculated sums of positive average daily temperatures for specific dates and altitudes, along with the determined melting coefficient, we established maximum snow reserve values at those altitudes.

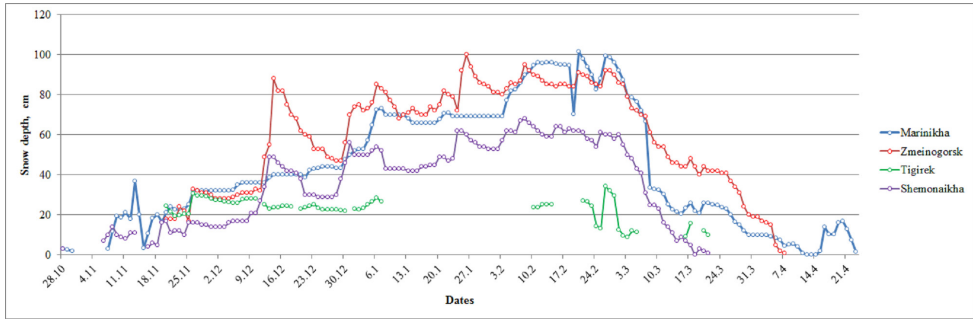


Figure 1. Snow depth (cm) during the winter period of 2022–2023 at weather stations in Zmeinogorsk (Russia), Shemonaikha (Kazakhstan), and observation sites of the Tigirek Nature Reserve (Russia) at the Tigirek and Marinikha cordons.

Table 1. Calculation of the coefficient of melting of snow cover in water equivalent per one degree of positive average daily air temperatures at the Zmeinogorsk weather station for 2013–2021

| Years | Period | | Water reserve, mm | | | The sum of the average daily temperatures for the period | Melting temperature coefficient, mm / (°C-day) | The amount of precipitation for the period, mm | The amount of precipitation during the period at subzero temperatures, mm | Melting temperature coefficient, mm/ (°C-day), considering solid precipitation |
|-------|--------|--------|-------------------|--------|---------------|--|--|--|---|--|
| | Date 1 | Date 2 | Date 1 | Date 2 | Melting layer | | | | | |
| 2013 | 05.Mar | 10.Mar | 198 | 182 | 16 | 2.9 | 5.5 | 29.1 | 6.3 | 7.7 |
| | 10.Mar | 15.Mar | 182 | 172 | 10 | 7.6 | 1.3 | 4.5 | 1.8 | 1.5 |
| | 15.Mar | 20.Mar | 172 | 122 | 50 | 4.8 | 10.4 | 8.2 | 5.5 | 11.6 |
| | 25.Mar | 31.Mar | 99 | 43 | 56 | 18.6 | 3.0 | 18.1 | 0 | 3.0 |
| | 31.Mar | 05.Apr | 43 | 41 | 2 | 6.2 | 0.3 | 17.8 | 14.1 | 2.6 |
| | 05.Mar | 05.Apr | 198 | 41 | 157 | 29.1 | 5.4 | 79.9 | 36.3 | 6.6 |
| 2014 | 15.Mar | 20.Mar | 108 | 61 | 47 | 14.2 | 3.3 | 8.2 | 0 | 3.3 |
| | 05.Mar | 20.Mar | 120 | 61 | 59 | 17.3 | 3.4 | 17.3 | 11 | 4.0 |
| 2015 | 20.Mar | 25.Mar | 156 | 90 | 66 | 10.6 | 6.2 | 14.1 | 0 | 6.2 |
| | 25.Mar | 31.Mar | 90 | 97 | -7 | 2.4 | - | 25.2 | 14.7 | 3.2 |
| | 20.Mar | 10.Apr | 156 | 78 | 78 | 13.3 | 5.9 | 35.5 | 21.4 | 7.5 |

| Years | Period | | Water reserve, mm | | | The sum of the average daily temperatures for the period | Melting temperature coefficient, mm / (°C-day) | The amount of precipitation for the period, mm | The amount of precipitation during the period at subzero temperatures, mm | Melting temperature coefficient, mm/ (°C-day), considering solid precipitation |
|-------|--------|--------|-------------------|--------|---------------|--|--|--|---|--|
| | Date 1 | Date 2 | Date 1 | Date 2 | Melting layer | | | | | |
| 2016 | 15.Mar | 20.Mar | 167 | 137 | 30 | 5.9 | 5.1 | 9.8 | 7 | 6.3 |
| | 25.Mar | 31.Mar | 137 | 51 | 86 | 20.6 | 4.2 | 19.2 | 0 | 4.2 |
| | 15.Mar | 31.Mar | 167 | 51 | 116 | 29.4 | 3.9 | 46 | 11.4 | 4.3 |
| 2017 | 25.Mar | 31.Mar | 128 | 47 | 81 | 22.6 | 3.6 | 14.1 | 0 | 3.6 |
| | 31.Mar | 05.Apr | 47 | 13 | 34 | 5.8 | 5.9 | 10.2 | 8.2 | 7.3 |
| | 25.Mar | 05.Apr | 128 | 13 | 115 | 26.1 | 4.4 | 22.5 | 8.2 | 4.7 |
| 2018 | 20.Mar | 31.Mar | 51 | 33 | 18 | 30.7 | 0.6 | 71.9 | 41.2 | 1.9 |
| | 20.Mar | 05.Apr | 51 | 35 | 16 | 30.7 | 0.5 | 73.3 | 42.6 | 1.9 |
| 2019 | 10.Mar | 15.Mar | 145 | 140 | 5 | 1 | 5.00 | 0 | 0 | 5.0 |
| | 25.Mar | 31.Mar | 152 | 83 | 69 | 17.1 | 4.0 | 3.5 | 3.5 | 4.2 |
| | 10.Mar | 31.Mar | 145 | 83 | 62 | 21.9 | 2.8 | 13.1 | 1.2 | 2.9 |
| 2020 | 10.Mar | 15.Mar | 310 | 306 | 4 | 4.5 | 0.9 | 4.8 | 4.1 | 1.8 |
| | 15.Mar | 20.Mar | 306 | 218 | 88 | 17.3 | 5.1 | 2.7 | 0 | 5.1 |
| | 20.Mar | 25.Mar | 218 | 173 | 45 | 6.7 | 6.7 | 8.2 | 0 | 6.7 |
| | 31.Mar | 05.Apr | 198 | 103 | 95 | 28.8 | 3.3 | 3.3 | 0 | 3.3 |
| | 05.Apr | 10.Apr | 103 | 14 | 89 | 30.9 | 2.9 | 5.2 | 0 | 2.9 |
| | 31.Mar | 10.Apr | 198 | 14 | 184 | 53.8 | 3.4 | 8.5 | 0 | 3.4 |
| | 15.Mar | 10.Apr | 310 | 14 | 296 | 78.9 | 3.7 | 30 | 4.8 | 3.8 |
| 2021 | 20.Mar | 25.Mar | 213 | 195 | 18 | 7.6 | 2.4 | 10 | 9 | 3.5 |
| | 25.Mar | 31.Mar | 195 | 187 | 8 | 3.3 | 2.4 | 31.8 | 12.4 | 6.2 |
| | 31.Mar | 05.Apr | 187 | 179 | 8 | 4.5 | 1.8 | 0 | 0 | 1.8 |
| | 05.Apr | 10.Apr | 179 | 62 | 117 | 23.7 | 4.9 | 5.4 | 0 | 4.9 |

The ecological impact of snow cover is significant, extending well beyond the winter season, particularly in areas where its quantitative characteristics are pronounced (Bykov et al. 2023; Kirdyanov et al. 2003). We further explored the influence of snow cover indicators on the radial growth of trees situated in elevations with substantial snow cover. For this investigation, we collected 30 cores from 15 trees at each site (Table 2), following established dendroclimatic methodologies (Shiyatov et al. 2000). Three tree-ring chronologies were developed from various sites (Bykov et al. 2022). In addition, we calculated the maximum snow reserves for the years 2013 to 2020 at the locations where these tree-ring chronologies were collected.

Table 2. Geographical location of the studied trees

| Species | Coordinates | | Absolute elevation of the terrain, m | Exposition | Slope |
|-------------------------------|-------------------|-------------------|--------------------------------------|------------|-------|
| | Northern latitude | Southern latitude | | | |
| <i>Larix sibirica</i> L. | 51.0862 | 83.0076 | 1286 | South-East | 2° |
| <i>Abies sibirica</i> L. | 51.0391 | 82.9593 | 1430 | East | 12° |
| <i>Pinus sibirica</i> Du Tour | 51.0451 | 82.9894 | 1535 | North-West | 6° |

Results and discussion

To calculate the snowmelt temperature coefficient for the snow cover, we utilized data from the Zmeinogorsk weather station, which included measurements of snowpack water equivalent along designated routes, daily precipitation amounts, and average daily air temperatures at a height of 2 meters, spanning the years 2013 to 2021. A total of 33 data cases were analyzed (see Table 1). Our findings indicate a strong correlation between the sums of average daily air temperatures and the corresponding snowmelt layers during the specified periods (Fig. 2), with a correlation coefficient of 0.88. This relationship can be leveraged, in conjunction with the altitudinal distribution of positive average daily air temperatures, to estimate snow reserves across varying elevations. However, this estimation faces limitations, particularly due to solid precipitation occurrences during the specified periods. Factoring in these precipitation events on days with negative average temperatures marginally improved the correlation between the examined parameters (Fig. 3). The melting temperature coefficient exhibited considerable variability, ranging from 0.3 to 10.4 mm/°C (Table 1). Notably, between March 25 and 31, 2015, one calculated instance even yielded a negative melt coefficient, as snow cover increased during this time. Nonetheless, the average coefficient was determined to be 3.7 mm/°C of positive average daily air temperature.

After accounting for atmospheric precipitation during periods when daily average air temperatures were negative, the revised average melt factor was found to be 4.3 mm/°C of daily average air temperature. This value was subsequently applied to compute snowpack water equivalents at various altitudes. The range of melt values for specific periods was substantial, oscillating between 1.8 and 11.6 mm (Table 1).

The computation of daily average air temperatures across different altitudes within the study area was facilitated by the high similarity in temperature profiles among several nearby meteorological stations surrounding the Tigiretsky Ridge. These included two state network stations—Shemonaikha (Kazakhstan, 320 m a.s.l.) and Zmeinogorsk (355 m a.s.l.)—as well as two stations from the Tigirek Reserve: Tigirek (480 m a.s.l.) and Babiy Klyuch (1530 m a.s.l.). The correlation coef-

ficients among the datasets from the first three meteorological stations ranged from 0.96 to 0.99.

The correlation coefficients between "Babiy Klyuch" and the "Tigirek" and "Zmeinogorsk" stations during the summer months ranged from 0.82 to 0.95, enabling us to reconstruct warm-season air temperature data (April to October) at this higher elevation using data from lower-elevation stations. However, correlations between the "Zmeinogorsk" and "Babiy Klyuch" stations during winter months were significantly weaker (Table 3), compromising the accuracy of adjusting Zmeinogorsk station data for Babiy Klyuch.

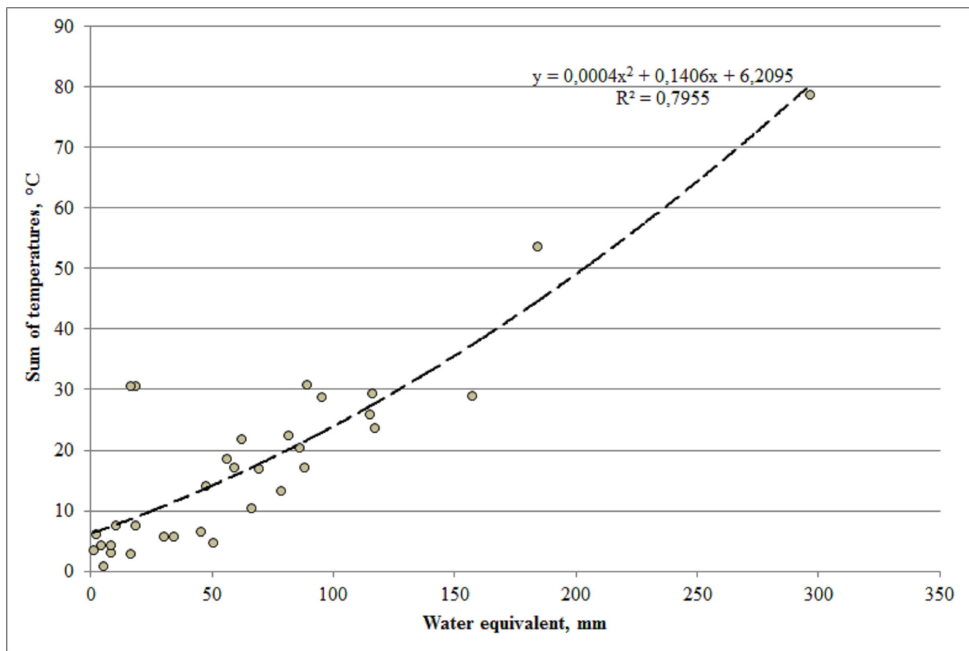


Figure 2. The dependence of snow cover melting on the sums of positive average daily air temperatures along the snow courses of weather station Zmeinogorsk from year 2013 to year 2021.

This relationship weakness can be attributed to several factors, including the presence of winter air temperature inversions, the icing of instruments during snowfall, and the immersion of sensors in accumulated snowpack due to significant snowfall and blizzard events. Nonetheless, during the spring and summer when snowmelt occurs, the correlation remains satisfactory.

After interpolating and extrapolating daily average air temperatures for various altitudes, cumulative temperature values were calculated for the satellite imagery acquisition dates—May 2, May 4, May 24, May 29, June 6, June 16, and July 3 (Table 4). To estimate the snowpack water equivalent, we applied a thermal melt factor of 4.3 mm for each degree of daily average positive air temperature (Table 5).

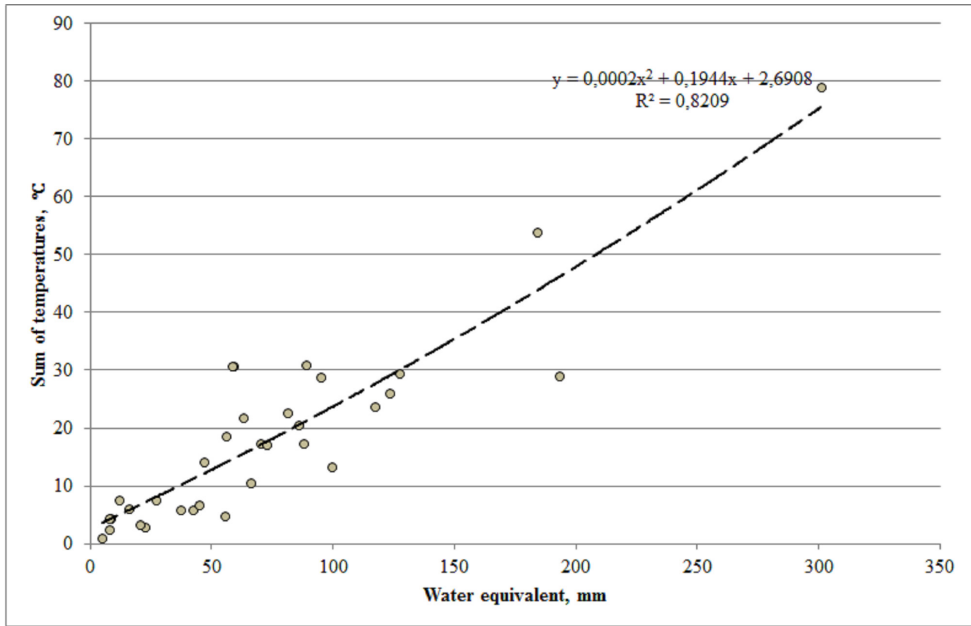


Figure 3. The dependence of snow cover melting on the sums of positive average daily air temperatures along the snow courses of weather station Zmeinogorsk from year 2013 to year 2021, taking into account the precipitation that occurred during periods of negative air temperatures.

Table 3. Regression relationship of average daily air temperatures at the Zmeinogorsk and Babiy Klyuch weather stations

| Month | The years used to construct the equation | The equation | Coefficient of determination |
|-----------|--|------------------------|------------------------------|
| | | | R ² |
| January | - | - | Below 0.3 |
| February | 2013, 2020, 2021 | $y = 0.5879x - 6.0837$ | 0.4943 |
| March | 2013, 2020, 2021 | $y = 0.8138x - 5.3819$ | 0.6135 |
| April | 2012, 2013, 2020, 2021 | $y = 0.8701x - 4.4912$ | 0.7851 |
| May | 2012, 2013, 2020 | $y = 1.0578x - 7.9718$ | 0.8199 |
| June | 2014, 2017, 2019 | $y = 1.1949x - 9.6022$ | 0.8634 |
| July | 2012, 2014, 2018–2020 | $y = 1.1251x - 7.9423$ | 0.7773 |
| August | 2012, 2016, 2018, 2019 | $y = 1.1x - 7.466$ | 0.7879 |
| September | 2012, 2016, 2018, 2019 | $y = 1.0001x - 5.328$ | 0.6575 |
| October | 2012, 2016, 2018, 2019 | $y = 0.9744x - 5.2394$ | 0.7357 |
| November | 2012, 2020 | $y = 0.5497x - 6.5685$ | 0.5039 |
| December | 2020 | $y = 0.5287x - 5.0891$ | 0.5901 |

Table 4. The sums of positive average daily air temperatures calculated for the Tigireki Ridge in 2021

| Elevation above sea level, m | The sum of the average daily air temperatures for specific dates | | | | | | |
|------------------------------|--|---------------------|----------------------|----------------------|----------------------|-----------------------|----------------------|
| | May 2 nd | May 4 th | May 24 th | May 29 th | June 6 th | June 16 th | July 3 rd |
| 500 | 162 | 181.6 | 430 | 513.1 | 643.3 | 792.4 | 1056.4 |
| 600 | 137.1 | 158.1 | 393.9 | 474.3 | 600.4 | 743.8 | 1000.5 |
| 700 | 120.9 | 139.9 | 363.5 | 443.5 | 564.3 | 704.8 | 955.5 |
| 800 | 105.7 | 122.9 | 336.8 | 413.7 | 531.9 | 666.9 | 911.5 |
| 900 | 92.7 | 108 | 312.6 | 386.1 | 501.6 | 631.1 | 869.7 |
| 1000 | 77.9 | 94.2 | 288.4 | 359.6 | 472.1 | 596.4 | 855.1 |
| 1100 | 68.1 | 82.2 | 266 | 334.9 | 444.0 | 563.5 | 821.2 |
| 1200 | 59.7 | 71.7 | 245.1 | 312.2 | 417.2 | 532.3 | 789.4 |
| 1300 | 51.9 | 62.4 | 226.6 | 290.8 | 393.2 | 503.2 | 758.8 |
| 1400 | 44.9 | 54.3 | 208.6 | 270.6 | 369.6 | 474.8 | 729.4 |
| 1500 | 38.6 | 46.9 | 191.5 | 251.1 | 346.7 | 447.2 | 700.8 |
| 1600 | 30.5 | 45.9 | 181.6 | 240.8 | 325.0 | 498.6 | 629.6 |
| 1700 | 28.4 | 43.3 | 170.1 | 227.0 | 307.2 | 480.8 | 604.1 |
| 1800 | 28.0 | 42.3 | 160.3 | 215.1 | 291.2 | 464.8 | 580.6 |
| 1900 | 29.1 | 42.9 | 152.4 | 204.9 | 277.0 | 450.6 | 559.1 |
| 2000 | 31.9 | 45.1 | 146.3 | 196.6 | 264.6 | 438.2 | 539.6 |

Table 5. The potential snowmelt layer calculated for the Tigiretsky Ridge by the Temperature-Based Melt-Index Method in 2021

| Elevation above sea level, m | The sum of the average daily air temperatures for specific dates | | | | | | |
|------------------------------|--|---------------------|----------------------|----------------------|----------------------|-----------------------|----------------------|
| | May 2 nd | May 4 th | May 24 th | May 29 th | June 6 th | June 16 th | July 3 rd |
| 500 | 697 | 781 | 1849 | 2206 | 2766 | 3407 | 4543 |
| 600 | 590 | 680 | 1694 | 2039 | 2582 | 3198 | 4302 |
| 700 | 520 | 602 | 1563 | 1907 | 2426 | 3031 | 4109 |
| 800 | 455 | 528 | 1448 | 1779 | 2287 | 2868 | 3919 |
| 900 | 399 | 464 | 1344 | 1660 | 2157 | 2714 | 3740 |
| 1000 | 335 | 405 | 1240 | 1546 | 2030 | 2565 | 3677 |
| 1100 | 293 | 353 | 1144 | 1440 | 1909 | 2423 | 3531 |
| 1200 | 257 | 308 | 1054 | 1342 | 1794 | 2289 | 3394 |
| 1300 | 223 | 268 | 974 | 1250 | 1691 | 2164 | 3263 |
| 1400 | 193 | 233 | 897 | 1164 | 1589 | 2042 | 3136 |
| 1500 | 166 | 202 | 823 | 1080 | 1491 | 1923 | 3013 |
| 1600 | 131 | 197 | 781 | 1035 | 1397 | 2144 | 2707 |

| Elevation above sea level, m | The sum of the average daily air temperatures for specific dates | | | | | | |
|------------------------------------|--|---------------------|----------------------|----------------------|----------------------|-----------------------|----------------------|
| | May 2 nd | May 4 th | May 24 th | May 29 th | June 6 th | June 16 th | July 3 rd |
| 1700 | 122 | 186 | 731 | 976 | 1321 | 2067 | 2598 |
| 1800 | 120 | 182 | 689 | 925 | 1252 | 1999 | 2497 |
| 1900 | 125 | 184 | 655 | 881 | 1191 | 1938 | 2404 |
| 2000 | 137 | 194 | 629 | 845 | 1138 | 1884 | 2320 |

To produce a map indicating maximum snowpack water equivalent, we first constructed a snow cover distribution map (Fig. 4) for the specified dates. This distribution map highlights the complex geographic factors that affect snowpack formation. Notably, we observed the presence of a barrier shadow within the Tigirek-Insk depression, leading to earlier snowmelt in this area compared to equivalent altitudes along the southern slopes of the Tigiretsky Ridge. This pattern is consistent up to an elevation of 1000 meters above sea level. Conversely, on the northern macro-slope within the watershed area, snow cover persists longer, likely due to greater snowpack accumulation from blizzards and the formation of persistent snow patches. During the summer months, particularly in July and August, these patches contribute to hydrological processes and water availability in the region.

Fig. 5 illustrates the spatial distribution of snowpack water equivalent across the elevations of interest, revealing considerable asymmetry between the southern and northern slopes of the Tigiretsky Ridge. Specifically, at altitudes ranging from 500 to 1200 meters above sea level, the southern macro-slope exhibits higher snowpack water equivalents than its northern counterpart. However, this trend reverses at elevations between 1200 and 1500 meters, where the snowpack water equivalent on the northern macro-slope significantly exceeds that on the southern slope (Table 6). These findings align with the theoretical perspectives on asymmetrical snow distribution noted by V.P. Galakhov (2003).

Particularly noteworthy are the observations near the ridgelines, where snow-drift phenomena exacerbate the differences between slopes. For instance, during March 2021, maximum snowpack water equivalents measured at the southern macro-slope between 1800 and 2000 meters ranged from 120 to 125 mm, whereas the northern slope recorded values soaring between 3000 and 3700 mm or higher. Consequently, snow patches form on the northern slope near these ridgelines; some of these patches endure through the summer months and may even evolve into permanent snowfields in certain years. The thin snow cover and high wind conditions prevalent near the ridgelines on the southern macro-slope result in a lower upper timberline compared to the northern slope. The accumulation of significant snow-drifts after initial snowfall near ridgelines on the northern macro-slope ensures that soil remains thawed throughout winter. This diverse distribution of snow cover engenders various ecological niches near the ridgelines, each characterized by distinct hydrothermal soil conditions.

The analysis of tree-ring chronologies collected from the area yielded insights into the climate sensitivity of trees in this region, with values ranging from 0.26 to 0.35, and expressed population signal (EPS) values ranging from 0.85 to 0.98 (Table 7). These parameters are vital for understanding the influence of climate fluctuations on tree growth in this mountainous landscape. The sensitivity of tree-ring chronology, which reflects year-to-year variability with a satisfactory threshold of 0.3 or higher, indicates how responsive tree growth is to climatic variations. Furthermore, the EPS values suggest a robust representation of the tree population, deemed satisfactory when above 0.85, thus supporting the construction of credible site chronologies.

However, the chronologies associated with *Pinus sibirica* Du Tour, sampled between 100 and 150 meters from the watershed on the northern slope, exhibited weak performance, pointing to diverse local growth factors influencing tree development in this particular area.

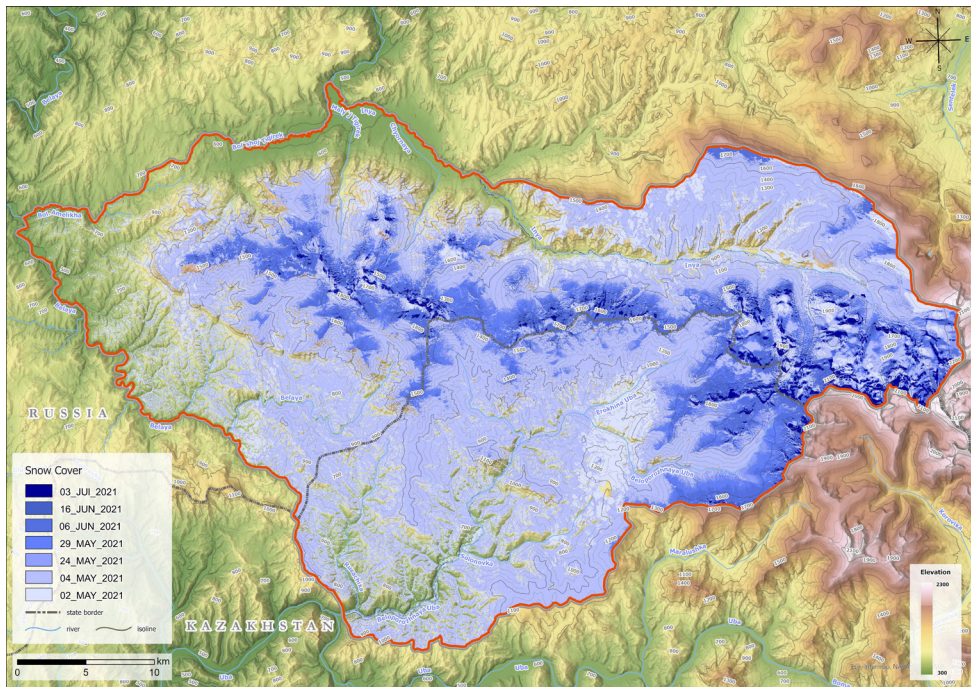


Figure 4. Position of snow cover on the Tigiretsky Range on specific dates in 2021.

Correlation analyses between tree-ring chronologies and meteorological data from Zmeinogorsk identified distinct climatic influences on various species. For *Larix sibirica* L., the radial increment was positively influenced by February precipitation and temperatures in June and July, while it showed a negative response to August temperatures. On the other hand, *Abies sibirica* L. demonstrated positive growth responses to June–July temperatures (especially in July) and adverse

responses to precipitation in May through August, particularly during July and August. For *Pinus sibirica*, June–July temperatures proved favorable for growth, while precipitation during May to August negatively impacted its radial increment.

Interestingly, the correlation between snowpack data from the Zmeinogorsk station and tree-ring chronologies was generally low. Statistically significant correlations were detected only for *Abies sibirica*, with maximum snowpack water equivalent values along the course of ($k = -0.27$) and snow depth in October ($k = -0.31$) (Table 8).

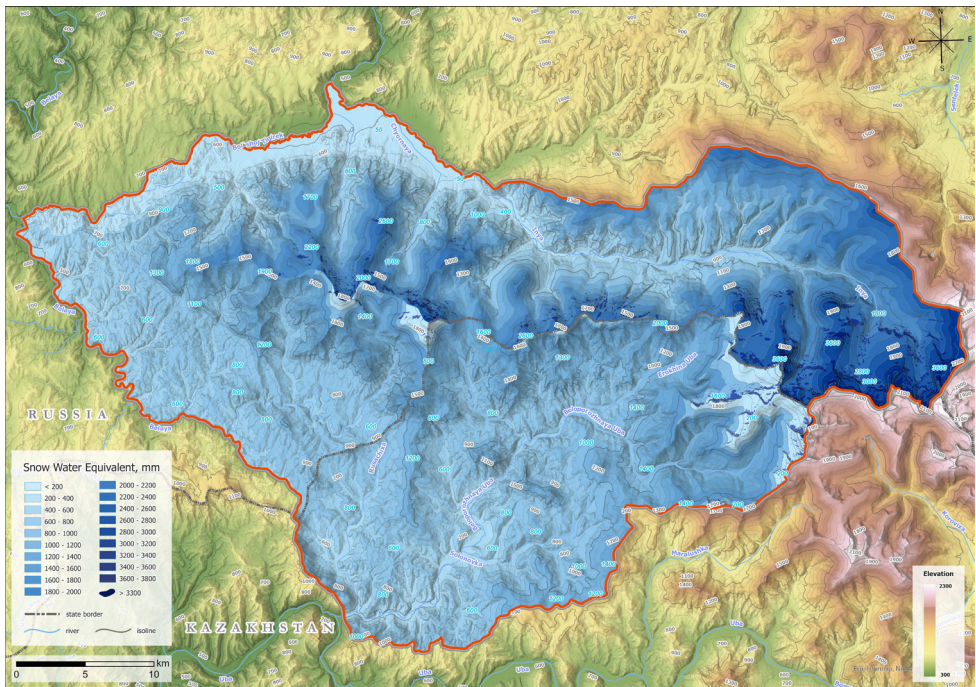


Figure 5. Maximum water content of snow cover on the Tigiretsky Range (Altai) in winter 2020–2021.

Given the weak correlation between the snowpack measurements at 355 meters above sea level and the tree-ring chronologies derived from higher elevations of 1300–1500 meters, we recalibrated the maximum snowpack water equivalent specifically for the areas from which dendrochronological samples were taken. This recalculation was constrained to the years 2013 to 2020, considering both the years of sample collection and the availability of satellite imagery. Despite the limited data, correlation analyses revealed a statistically significant relationship between the ring width indices of *Abies sibirica* and the maximum snowpack water equivalent at an altitude of 1500 meters above sea level. This finding suggests that an increase in the maximum snowpack water equivalent at this elevation indeed correlates with enhanced radial growth of *Abies sibirica* at altitudes of around 1400 meters.

In conclusion, the interplay between snowpack dynamics, altitude, and climate on the northern and southern slopes of the Tigiretsky Ridge outlines a complex ecological framework. Continued research on these dynamics is essential for improving our understanding of cryospheric processes and their implications for local ecology and hydrology.

Table 6. Distribution of snowpack water equivalent (mm) in 2021 on the northern and southern macroslopes of the Tigireki Range

| Absolute elevation of the terrain, m | The northern macroslope | The southern macroslopes |
|--------------------------------------|-------------------------|--------------------------|
| 500 | 54 | 300 |
| 600 | 63 | 500 |
| 700 | 259 | 602 |
| 800 | 455 | 737 |
| 900 | 464 | 872 |
| 1000 | 757 | 1008 |
| 1100 | 1049 | 1144 |
| 1200 | 1342 | 1342 |
| 1300 | 1691 | 1392 |
| 1400 | 1807 | 1442 |
| 1500 | 1923 | 1491 |
| 1600 | 2261 | 838 |
| 1700 | 2600 | 186 |
| 1800 | 2993 | 120 |
| 1900 | 3324 | 125 |
| 2000 | 3669 | 125 |

Table 7. Average correlation coefficient, expressed population signal и sensitivity site chronology

| Tree species | Average correlation coefficient chronology | Expressed population signal | Sensitivity of site standardized TRC |
|-------------------------------|--|-----------------------------|--------------------------------------|
| <i>Larix sibirica</i> L. | 0.24 | 0.93 | 0.35 |
| <i>Abies sibirica</i> L. | 0.59 | 0.98 | 0.30 |
| <i>Pinus sibirica</i> Du Tour | 0.16 | 0.85 | 0.26 |

Table 8. Correlation coefficients of the series of the maximum snowpack water equivalent (mm) and the indices of the ring width of site chronologies for 2013–2020

| Tree ring chronology | Maximum snowpack water equivalent | | |
|---|-----------------------------------|--------|--------|
| | 1300 m | 1400 m | 1500 m |
| Chronology of <i>Larix sibirica</i> L. | -0.11 | -0.47 | -0.26 |
| Chronology of <i>Abies sibirica</i> L. | 0.25 | 0.63 | 0.81 |
| Chronology of <i>Pinus sibirica</i> Du Tour | 0.27 | 0.00 | 0.19 |

Conclusion

The Temperature-Based Melt-Index Method facilitates the accurate determination of maximum snowpack water equivalent during the winter months. An ecological and geographical interpretation of the acquired snow cover data enables the identification of differentiation patterns across the study area, influenced by factors such as elevation, slope aspect, and distance from watersheds. This approach also initiates the exploration of relationships within the snow cover-river runoff and snow cover-vegetation systems.

Our findings reveal an asymmetrical altitudinal distribution of snow cover on the northern and southern slopes of the Tigiretsky Ridge. Specifically, at elevations between 500 and 1200 meters, maximum snow reserves are greater on the southern slope, while higher elevations see an increase in snow reserves on the northern slope. The most pronounced differences in snow cover distribution between the slopes occur near watersheds, where snow reserves on the northern slope can exceed those on the southern slope by a factor of up to 30.

Additionally, the radial growth of trees responds variably to snow cover indicators, influenced by both the trees' locations and their species composition. Notably, an increase in maximum snowpack water equivalent has been shown to positively affect the radial increment of *Abies sibirica* near the ecotone of the upper timberline. Future research should aim to uncover the underlying reasons for this relationship and to validate these findings through extended observation periods.

Acknowledgements

This work has been funded by the Science Committee of the Ministry of Science and Higher Education of the Republic of Kazakhstan (Grant No. BR24992899).

References

- Ahlmann HW (1924) Le Niveau De Glaciation Comme Fonction De L'accumulation D'humidité Sous Forme Solide: Méthode Pour Le Calcul De L'Humidité Condensée Dans La Haute Montagne Et Pour L'étude De La Fréquence Des Glaciers. *Geografiska Annaler* 6(3–4): 223–272. <https://doi.org/10.1080/20014422.1924.11881098>
- Braithwaite R J (1981) On glacier energy balance, ablation, and air temperature. *Journal of Glaciology* 27: 381–391.
- Bykov NI, Shigimaga AA, Sabaev AA (2022) Features of radial growth of woody plants in the upper part of the mountain forest belt of the Tigiretsky Ridge. *Proceedings of the Tigirek Nature Reserve* 14-1 (14): 29–34. [In Russian]
- Bykov NI, Rygalova NV, Shigimaga AA (2024) Dendrochronological analysis of snow avalanches in the Northwestern Altai (Korgon river basin). *Ice and Snow* 64 (1): 081–095. <https://doi.org/10.31857/S2076673424010066> [In Russian]
- Bykov NI, Shigimaga AA, Rygalova NV (2023) Response of the Radial Growth of Woody Plants in the West Siberian Plain and Adjacent Mountainous Territories to the Characteristics of the Snow Cover. *Forests* 14(8):1690. <https://doi.org/10.3390/f1408169>
- Bykov NI, Sabaev AA, Davydov EA, Kasurov DA (2021) Observations of nival-glacial phenomena in the Tigirek State. In: *Geographical research of Siberia and the Altai-Sayan transboundary region*. Publishing House of Altai State University, Barnaul, 126–134. [In Russian]
- Galakhov VP (2003) Conditions of formation and calculation of maximum snow reserves in the mountains (Based on the results of research in Altai). Publishing house «Nauka», Novosibirsk, 104 pp. [In Russian]
- Egorina AV (2003) Barrier factor in the formation of the natural environment of the city. Publishing House of Altai State University, Barnaul, 344 pp. [In Russian]
- Egorina AV, Revyakin VS (2022) The Mongolian-Siberian anticyclone in the fate of nomadic civilizations of Eurasia. Publishing House "VKPK ARGO", Ust-Kamenogorsk, 252 pp. [In Russian]
- Glaciological Dictionary (1984) Publishing house «Hydrometeoizdat», Leningrad, 526 pp. [In Russian]
- Hann J (1908) *Handbuch der Klimatologie (Handbook of Climatology)*. Verlag von J. Engelhorn, 394 pp.
- Iglovskaya NV, Narozhny YuK (2010) Determination of snow reserves in Altai using satellite information. *Bulletin of Tomsk State University* 334: 160–165. [In Russian]
- Hall DK, Riggs GA, Salomonson VV (1995) Development of methods for mapping global snow cover using moderate resolution imaging spectroradiometer data. *Remote Sensing of Environment* 54(2): 127–140. [https://doi.org/10.1016/0034-4257\(95\)00137-P](https://doi.org/10.1016/0034-4257(95)00137-P)
- Hall DK, Riggs GA (2011) Normalized-Difference Snow Index (NDSI). In: Singh VP, Singh P, Haritashya UK (Eds) *Encyclopedia of Snow, Ice and Glaciers*. Encyclopedia of Earth Sciences Series. Springer, Dordrecht, 779–780. https://doi.org/10.1007/978-90-481-2642-2_376

- Hawker L, Uhe P, Paulo L, Sosa J, Savage J, Sampson C, Neal J (2022) A 30 m global map of elevation with forests and buildings removed. *Environmental Research Letters* 17 (2): 24016. <https://doi.org/10.1088/1748-9326/ac4d4f>
- Hao X, Huang G, Zheng Z, Sun X, Ji W, Zhao H, Wang J, Li H, Wang X (2022) Development and validation of a new MODIS snow-cover-extent product over China. *Hydrology and Earth System Sciences* 26: 1937–1952. <https://doi.org/10.5194/hess-26-1937-2022>
- Hock R (1999) A distributed temperature-index ice- and snowmelt model including potential direct solar radiation. *Journal of Glaciology* 45(149): 101–111. <https://doi.org/10.3189/S0022143000003087>
- Jiang L, Yang J, Zhang C, Wu S, Li Z, Dai L, Li X, Qiu Y (2022) Daily snow water equivalent product with SMMR, SSM/I and SSMIS from 1980 to 2020 over China. *Big Earth Data* 6(4): 420–434. <https://doi.org/10.1080/20964471.2022.2032998>
- Climate of Ust-Kamenogorsk (ecological and geographical aspect) (2009) Ust-Kamenogorsk, 240 pp. [In Russian]
- Kotlyakov VM, Khodakov VG, Grinberg AM (1981) Thermal manifestation of snow and ice objects as a method of quantitative interpretation of aerospace information. *Bulletin of the USSR Academy of Sciences. Geographical Series* 3: 127–132. [In Russian]
- Krenke AN, Khodakov VG (1966) On the relationship of surface melt of glaciers with air temperature. *Data of glaciological studies (Chronicle Discussions)* 12: 153–164. [In Russian]
- Kirdyanov A, Hughes M, Vaganov E, Schweingruber F, Silkin P (2003) The importance of early summer temperature and date of snow melt for tree growth in the Siberian Subarctic. *Trees* 17: 61–69. <https://doi.org/10.1007/s00468-002-0209-z9-z>
- Lang H (1978) Relations between glacier runoff and meteorological factors observed on and outside the glacier. *IAHS Publ* 79: 429–439.
- Lang H, Braun L (1990) On the information content of air temperature in the context of snow melt estimation. *Hydrology of Mountainous Areas, IAHS*, 347–354.
- Nefedeva EA, Yashina AV (1985) The role of snow cover in differentiation of the landscape sphere. Publishing house «Nauka», Moscow, 144 pp. [In Russian]
- Ohmura A (2001) Physical Basis for the Temperature-Based Melt-Index Method. *Journal of Applied Meteorology (1988–2005)* 40(4): 753–761. [https://doi.org/10.1175/1520-0450\(2001\)040<0753:PBFTTB>2.0.CO;2](https://doi.org/10.1175/1520-0450(2001)040<0753:PBFTTB>2.0.CO;2)
- Reeh N (1989) Parameterization of melt rate and surface temperature on the Greenland ice sheet. *Polarforschung* 59: 113–128.
- Revyakin VS, Kravtsova VI (1977) Snow cover and avalanches of Altai. Publishing house of Tomsk State University, Tomsk, 215 pp. [In Russian]
- Revyakin VS (1981) Natural ice of the Altai-Sayan mountain region. Publishing house «Gidrometeoizdat», Leningrad, 288 pp. [In Russian]
- Shiyatov SG, Vaganov EA, Kirdyanov AV, Kruglov VB, Mazepa VS, Naurzbayev MM, Khantemirov RM (2000) Methods in Dendrochronology. Part 1: Fundamentals of Dendrochronology. *Collection of Tree-Ring Data. Krasnoyarsk*, 80 pp. [In Russian]

Chernykh DV, Samoylova GS (2011) Landscapes of Altai (Altai Republic and Altai Krai) Map M-1:500000. Publishing house of Novosibirsk Cartographic Factory, Novosibirsk. [In Russian]

Zschenderlein L, Luojus K, Takala M, Venäläinen P, Pulliainen J (2023) Evaluation of passive microwave dry snow detection algorithms and application to SWE retrieval during seasonal snow accumulation. Remote Sensing of Environment 288: 113476. <https://doi.org/10.1016/j.rse.2023.113476>